European Journal of Pharmaceutics and Biopharmaceutics 137 (2019) 1–8

Contents lists available at ScienceDirect

European Journal of Pharmaceutics and Biopharmaceutics

journal homepage: www.elsevier.com/locate/ejpb

Research paper

Ultrasound-responsive nanobubble-mediated gene transfection in the cerebroventricular region by intracerebroventricular administration in mice

Koki Ogawa[a], Yuki Fuchigami[a], Masayori Hagimori[a], Shintaro Fumoto[a], Kazuo Maruyama[b], Shigeru Kawakami[a,*]

[a] Graduate School of Biomedical Sciences, Nagasaki University, 1-7-1 Sakamoto, Nagasaki-shi, Nagasaki 852-8588, Japan
[b] Faculty of Pharma-Sciences, Teikyo University, 2-11-1 Kaga, Itabashiku, Tokyo 173-8605, Japan

ARTICLE INFO

Keywords:
Gene delivery
Intracerebroventricular injection
Ultrasound
Choroid plexus
plasmid DNA
Nanobubbles

ABSTRACT

Aim: Intracerebroventricular (ICV) administration of ultrasound-responsive bubbles and cranial ultrasound irradiation is reported as a transfection system for the cerebroventricular region. This study aimed to characterize the transfection system with respect to transfection efficiency, spatial distribution of transgene expression, and safety.

Methods: Plasmid DNA was transfected to mouse brain by ICV injection of ultrasound-responsive nanobubbles, followed by ultrasound irradiation to brain. Spatial distribution of transgene expression in the cerebroventricular region was investigated using multicolor deep imaging.

Result: This transfection system efficiently transferred the transgene to the choroid plexus with no morphological change or cerebral hemorrhage. Moreover, sustained secretion of transgenic protein was achieved by transferring the transgene encoding the secretable protein.

Conclusion: We successfully developed an ultrasound-responsive nanobubbles-mediated method for gene transfection into the cerebroventricular region via ICV administration in mice.

1. Introduction

Endogenous neural stem cells (NSCs) at subventricular zone (SVZ) are potential therapeutic targets for neurological diseases because they generate new neurons or glial cells in the adult brain [1–3]. It has been reported that the intracerebroventricular (ICV) infusion of mitogenic proteins, such as growth factors or neurotrophic factors, into the lateral ventricle activated neurogenesis in the SVZ [4]. However, translating this therapeutic approach to a clinical application may be very challenging because continuous protein infusion into the lateral ventricle over several days was required to activate NSCs and promote neurogenesis [4], due to the instability of the protein.

On the other hand, genetically modifying the cells at the SVZ using gene vectors such as plasmid DNA (pDNA) is expected to exhibit long therapeutic effects over protein because transfected genes exert longer bioeffects than proteins. Taking this into consideration, therapeutic gene transfection to the lateral ventricle tissue may be a promising approach for treatment of several cerebral disorders. Since pDNA alone has low transfection ability, several carriers for promoting transfection have been proposed. Polyplexes, which are complexes of pDNA and cationic polymers such as polyethyleneimine (PEI) are known as transfection carriers for the SVZ via ICV administration [5,6]. Although polyplexes are powerful carriers to cells surrounding the lateral ventricle, they are reported to have neurotoxicity and cause inflammation in the peri-ventricular area because of their high positive surface charge [7].

Ultrasound-responsive bubbles combined with ultrasound irradiation are reported to transfer pDNA with high efficiency and safety *in vivo* by generated cavitation energy [8]. Our group has developed several types of ultrasound-responsive gene carriers such as lipid-based bubbles with naked pDNA [9–11], bubble lipoplexes [12], and bubble lipopolyplexes [13]. We applied bubble lipopolyplexes for efficient and safe transfection to the brain by intravenous injection and ultrasound irradiation [14].

Recently, ultrasound-mediated gene transfection has been applied to the cerebroventricular region in combination with ICV administration of bubbles. Tan et al [15] have reported efficient gene expression at the SVZ by ICV administration of microbubbles and polyplexes following by ultrasound irradiation to brain. They first demonstrated the proof of concept of the ultrasound-mediated gene transfection to the

* Corresponding author at: Department of Pharmaceutical Informatics, Graduate School of Biomedical Sciences, Nagasaki University, Nagasaki, Japan.
E-mail addresses: y-fuchigami@nagasaki-u.ac.jp (Y. Fuchigami), hagimori@nagasaki-u.ac.jp (M. Hagimori), sfumoto@nagasaki-u.ac.jp (S. Fumoto), maruyama@pharm.teikyo-u.ac.jp (K. Maruyama), skawakam@nagasaki-u.ac.jp (S. Kawakami).

https://doi.org/10.1016/j.ejpb.2019.02.003
Received 14 November 2018; Received in revised form 5 February 2019; Accepted 6 February 2019
Available online 07 February 2019
0939-6411/

cerebroventricular region. In terms of the transfection efficacy and safety, the combination of ICV administration of bubbles and ultrasound irradiation is expected to be a superior gene transfection system to conventional polyplex systems. However, to the best of our knowledge, there is only one study that applied bubbles and ultrasound for gene transfection to the cerebroventricular region. Therefore, it is necessary to further develop the transfection system in terms of the optimal ultrasound condition, transfection efficiency, distribution of transgene expression, and safety because this information is essential for therapeutic application.

The distribution of transgene expression is highly important information for therapeutic application because we cannot identify the therapeutic gene if the distribution is unclear. Tan et al [15] evaluated the transgene distribution obtained by microbubbles and ultrasound using immunostaining of tissue sections. Although tissue sectioning is a widely-used method for evaluating transgene distribution, it can provide only 2-dimensional (2D) images. Precisely observing the transgene expression and anatomical structure is difficult with 2D imaging because several tissues such as the ventricle wall, capillaries, and choroid plexus are sterically confused in the cerebroventricular region. To obtain 3D images for comprehensive observation, we previously developed a multicolor deep imaging system using a tissue-clearing method and confocal microscopy [11,14,16–19]. Recently, we have evaluated the positional relationship of the transgene expression and cerebral vessels simultaneously in the brain by vascular staining with lipophilic dyes [14]. Taking these into consideration, we expect that the distribution of transgene expression in cerebroventricular region can be clarified using multicolor deep imaging.

In this study, we developed a method for ultrasound-mediated transfection to the cerebroventricular region for therapeutic application. NBs with naked pDNA (pDNA + NBs) and bubble lipopolyplexes were used as ultrasound-responsive gene carriers because they have a non-cationic surface charge. We administered these carriers into the lateral ventricles of mice via ICV injection followed by ultrasound irradiation to the brain. First, we measured the transgene expression under various ultrasound conditions to evaluate the effect of the ultrasound condition on expression, and then we established an optimal transfection condition. Next, transfection efficiency of the ultrasound-responsive carriers was compared with that of the conventional transfection carrier, PEI polyplexes. Then, we investigated the spatial transgene distribution by visualizing the anatomical structures in the cerebroventricular region using multicolor deep imaging. We eventually revealed that transgene expression was located at the choroid plexus, which is responsible for producing cerebrospinal fluid (CSF). Finally, we confirmed the sustained expression of secretory transgenic protein into CSF for a possible therapeutic approach.

2. Materials and methods

2.1. Materials

The chemicals, 1,2-Distearoyl-sn-glycero-3-phosphocholine (DSPC) and 1,2-distearoyl-sn-glycero-3-phospho-(1′-rac-glycerol) (DSPG), were purchased from Avanti Polar Lipids Inc. (Alabaster, AL, USA). N-(Carbonyl-methoxypolyethyleneglycol 2000)-1,2-distearoyl-sn-glycero-3-phosphoethanolamine (mPEG-DSPE) was purchased from NOF Co. (Tokyo, Japan). 4′,6-Diamidino-2-phenylindole (DAPI), 1,1′-dioctadecyl-3,3,3′,3′-tetramethylindocarbocyanine perchlorate (DiI), polyethyleneimine (PEI) (branched, 25 kDa) and protamine sulfate were purchased from Sigma-Aldrich Co. (St. Louis, MO, USA). Sorbitol, paraformaldehyde (PFA), urea, and dimethyl sulfoxide were purchased from Wako Pure Chemical Industries, Ltd. (Osaka, Japan). Glycerol was purchased from nakalai tesque (Kyoto, Japan).

2.2. Animal

Five-week-old male ddY mice (25–30 g) were purchased from Japan SLC, Inc. (Hamamatsu, Japan), housed in cages in an air-conditioned room, and maintained on a standard laboratory diet (MF; Oriental Yeast Co., Ltd., Tokyo, Japan) with food and water available *ad libitum*. All animal experiments were performed in accordance with the guideline for animal experimentation of Nagasaki University, and approved by the Institutional Animal Care and Use Committee of Nagasaki University (approval number: 1308051086-6).

2.3. pDNA

pCMV-Luc was constructed as reported previously [20]. pZsGreen1-N1 was purchased from Clontech (Takara Bio Inc., Shiga, Japan). pCpGfree-Lucia, which is completely devoid of CpG dinucleotides, was purchased from Invivogen (SanDiego, CA, USA). pDNA was amplified in *E. coli* and purified using an EndoFree® Plasmid Giga kit (QIAGEN GmbH, Hilden, Germany).

2.4. Preparation of NBs, bubble lipopolyplexes, polyplexes

NBs composed of DSPC and mPEG-DSPE (94:6 (m/m)) were prepared as previously described [11,21]. Briefly, DSPC and mPEG-DSPE were dissolved in methanol (94:6 in a molar ratio). After evaporation and desiccation, lipid film was hydrated at 65 °C in phosphate buffer saline to produce liposome. The liposome was sonicated for 3 min using a tip sonicator. To encapsulate C_3F_8 gas, liposome was vigorously shaken in a bath-type sonicator.

Bubble lipopolyplexes composed of pDNA, protamine sulfate, and anionic liposome (1:1.5:7 (w/w)) were prepared as previously described [14]. To prepare anionic liposome, DSPG, DSPC, and mPEG-DSPE was dissolved in methanol (7:2:1 in a molar ratio). After evaporation and desiccation, lipid film was hydrated at 65 °C in 5% glucose. The dispersion was sonicated for 10 min using a bath sonicator, and then sonicated in a tip sonicator for 3 min. To prepare the complex of pDNA, protamine sulphate, and anionic liposome, pDNA and protamine sulphate were mixed in 5% glucose solution and incubated for 15 min. Anionic liposome was added to the mixture of pDNA and protamine sulfate, and incubated for 15 min. After that, saline was added to the formulation to give the final NaCl concentration of 6 mM. To encapsulate C_3F_8 gas, formulation was vigorously shaken in a bath-type sonicator. Particle size and zeta-potential of bubble formations were measured with Zetasizer Nano ZS (Malvern Instruments, Malvern, UK) as previously described [14].

For preparation of polyplexes, pDNA and PEI were dissolved in 5% glucose solution. Each component was mixed at charge ratio of 6. Complexes were then incubated for 15 min before administration.

2.5. ICV injection

Mice were anesthetized with three types of mixed anesthetic agents prepared as described [22], and scalp fur was removed. 5 μL of each formulation was injected into the lateral ventricle (1 mm lateral and 0 mm caudal to bregma) using a two-step injection needle connected to a 50 μL Hamilton syringe via a polyethylene tube with an inner diameter of 0.35 mm. Each formulation was injected over 30 sec. After injection, the needle was kept in place for 30 sec to prevent backflow.

2.6. In vivo transfection

For polyplex-mediated transfection, 5 μL of polyplexes (0.625 μg, in terms of pDNA) was administered into the left ventricle via ICV injection, as mentioned above. For ultrasound-mediated transfection, a mixture of pDNA (0.625 μg) and NBs (4.375 μg), or bubble lipopolyplexes (0.625 μg, in terms of pDNA) was administered into the left

ventricle via ICV injection as described above. One min after injection, ultrasound was transdermally irradiated the head using a Sonopore-4000 sonicator (NEPA GENE, Chiba, Japan) using a probe with a diameter of 20 mm.

2.7. Luciferase assay

Six hours after transfection of pCMV-Luc, brains and other organs were harvested. Brains were dissected into the olfactory bulb (OB), left hemisphere (LH), right hemisphere (RH), and hindbrain (HB), referencing the literature [23] as necessary. The dissected area is illustrated in Fig. 2D. Firefly luciferase activity was measured according to the previous report [16].

To evaluate the sustained lucia secretion, we measured the lucia level in CSF and serum at various times after transfection of pCpGfree-Lucia. CSF was collected from the cisterna magna as described [24]. Lucia expression in CSF and serum was measured using QUANTI-Luc according to the manufacturer's instructions.

2.8. Multicolor deep imaging

We evaluated the spatial distribution of ZsGreen1 expression with multicolor deep imaging utilizing tissue clearing. Twenty-four hours after transfection of pZsGreen1-N1, brain tissues were fixed with 4% PFA. Next, brains were coronally sliced at bregma in approximately 2-mm-thickness, then cleared with Sca*l*eSQ, containing DAPI (5 μg/mL) for nuclear staining. The procedure of tissue clearing with Sca*l*eSQ was performed as described in the literature [25]. To visualize the ventricle walls, DiI (2 mg/mL in dimethyl sulfoxide) was injected into the right lateral ventricle at 6 h before the fixation. To visualize the blood vessels, vascular staining was performed as described [26].

Left ventricular area of cleared tissues were observed with a confocal laser microscope (LSM 710; Carl Zeiss Microimaging GmbH, Jena, Germany) equipped with ×10 dry or ×40 oil-immersion objective lenses, and Z-stack images were obtained. DAPI, ZsGreen1 and DiI were excited by lasers at 405, 493 and 549 nm respectively. The acquisition software was ZEN2012.

2.9. Histological assessment

Twenty-four hours after transfection of pZsGreen1-N1, mice were fixed with 4% PFA. Brains were embedded in paraffin. The samples were sectioned at 5 μm using a microtome (Microm HM355S; Thermo Fisher Scientific, Waltham, MA, USA) and stained with hematoxylin and eosin (HE). After HE stain, the region around the left lateral ventricle was observed using an AxioVert A1 microscope (Carl Zeiss Meditec AG, Jena, Germany) equipped with a ×10 dry objective lens.

2.10. Statistical analysis

Statistical comparisons were performed by Student's *t*-test (two-tailed) for two groups and Tukey's test for multiple groups. *P*-values of less than 0.05 were considered statistically significant.

3. Results

3.1. Physicochemical properties of bubble formulations

The average particle size of NBs and bubble lipopolyplexes was 359 ± 12.6 nm and 407 ± 33.1 nm respectively (Data represent the mean ± SD of three experiments.). Zeta-potential of NBs and bubble lipopolyplexes was −1.60 ± 0.39 mV and –22.9 ± 2.27 mV respectively (Data represent the mean ± SD of three experiments.). These values are corresponding with our previous reports about nanobubbles [11,21] and bubble lipopolyplexes [14].

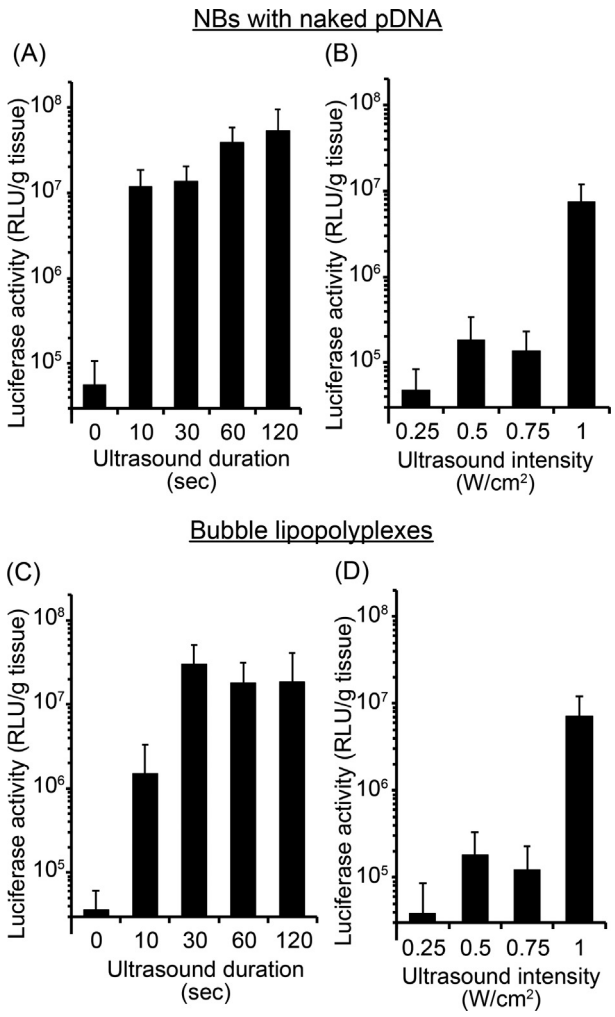

Fig. 1. Effect of ultrasound irradiation condition on the transgene expression. (A, C) Mice were administered pDNA + NBs (A) or bubble lipopolyplexes (C) and irradiated with ultrasound for 0, 10, 30, 60, and 120 sec at 1 W/cm^2. (C, D) Mice were administered pDNA + NBs (B) or bubble lipopolyplexes (D) and irradiated with ultrasound for 60 sec at 0.25, 0.5, 0.75, and 1 W/cm^2. Six hours after transfection, luciferase expression in murine whole brains was measured. Data represent means ± SD. Abbreviation: NBs, nanobubbles; SD, standard deviation; RLU, relative light unit.

3.2. The effect of ultrasound condition on transfection efficiency

To evaluate the effect of ultrasound duration and intensity on the transfection efficiency in the cerebroventricular region, mice were irradiated with several conditions of ultrasound followed by ICV administration of pDNA + NBs and bubble lipopolyplexes. First, ultrasound irradiation was performed for 0, 10, 30, 60, and 120 sec followed by ICV administration of pDNA + NBs or bubble lipopolyplexes. In both carriers, transgene expression was increased as the irradiated duration increased, up to 60 sec (Fig. 1A and C). After 60 sec of ultrasound irradiation, transgene expression was plateaued (Fig. 1A and C). Next, ultrasound irradiation was performed at 0.25, 0.5, 0.75, and 1 W/cm^2 followed by ICV administration of pDNA + NBs or bubble lipopolyplexes. Low transgene expression was observed in both carriers when brains were irradiated under 0.75 W/cm^2 (Fig. 1B and D). On the other hand, when ultrasound intensity was 1 W/cm^2, transgene expression was drastically increased (Fig. 1B and D).

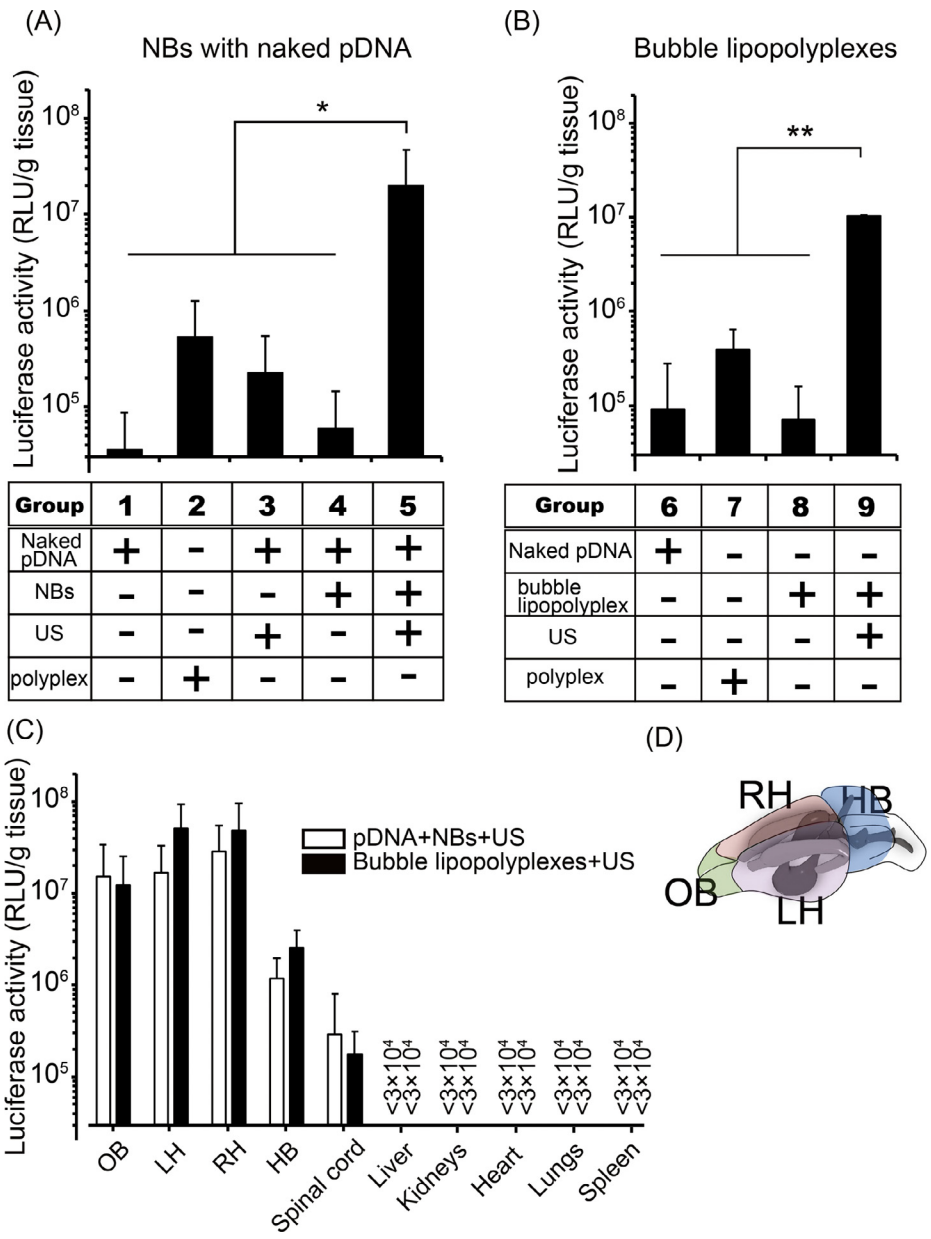

Group	1	2	3	4	5
Naked pDNA	+	-	+	+	+
NBs	-	-	-	+	+
US	-	-	+	-	+
polyplex	-	+	-	-	-

Group	6	7	8	9
Naked pDNA	+	-	-	-
bubble lipopolyplex	-	-	+	+
US	-	-	-	+
polyplex	-	+	-	-

Fig. 2. Transgene expression by each transfection method. (A) Mice were administered several carriers, then ultrasound irradiation was performed for 60 sec at 1 W/cm^2 to the brains of mice in the ③pDNA + US and ⑤pDNA + NBs + US groups. Six hours after transfection, luciferase expression in the mouse whole brains were measured. (n = 7) Data represent means ± SD. *P < 0.05 by Tukey's test. (B) Mice were administered several carriers, followed by ultrasound irradiation for 60 sec at 1 W/cm^2 to the brains of mice in the ⑨bubble lipopolyplexes + US group. Six hours after transfection, luciferase expression in the whole mouse brains were measured. (n = 6) Data represent means ± SD. **P < 0.01 by Tukey's test. (C) Transgene expression level in each area of brain. Six hours after luciferase transfection by pDNA + NBs or bubble lipopolyplexes combined with ultrasound irradiation, luciferase expression in each area of brain, spinal cord, liver, kidneys, heart, lungs, and spleen was measured (n = 4). Brains were dissected into OB, RH, LH, and HB as illustrated in (D). Data represent means ± SD. There was no difference between pDNA + NBs + US and bubble lipopolyplexes + US at all brain areas in Student's t-test. Abbreviation: pDNA, plasmid DNA; US, ultrasound; NBs, nanobubbles; PEI, polyethylenimine; OB, olfactory bulb, LH, left hemisphere; RH, right hemisphere; HB, hindbrain; SD, standard deviation; RLU, relative light unit.

3.3. Efficiency of ultrasound-mediated transfection to the lateral ventricle

We evaluated the transfection efficacy of pDNA + NBs and bubble lipopolyplexes combined with ultrasound, and then compared them with the efficacy of conventional carriers, PEI polyplexes. In Fig. 2A, transgene expression of pDNA + NBs combined with ultrasound irradiation was significantly higher than relevant other groups; pDNA, PEI polyplexes, pDNA + US, and pDNA + NBs. Similarly, transgene expression of bubble lipopolyplexes combined with ultrasound was also significantly higher than for other groups; pDNA, PEI polyplexes, and bubble lipopolyplexes (Fig. 2B).

Next, to roughly evaluate the transfected area in the nervous system, brains and spinal cords were harvested, and brains were divided into OB, LH, RH, and HB as illustrated in Fig. 2D. Fig. 2C shows the transgene expression level transfected by pDNA + NBs or bubble lipopolyplexes in each area of the brain and other organs. Transgene expression was observed mainly in OB, LH and RH, rather than in the HB and spinal cords (Fig. 2C). Moreover, transgene expression was restricted to the brains and spinal cords, and was not detected in other organs such as the liver, kidneys, heart, lungs or spleen (Fig. 2C).

3.4. Spatial transgene distribution

In order to evaluate the spatial distribution of transgene expression, we observed the ZsGreen1-transfected cerebroventricular region with multicolor deep imaging utilizing tissue clearing. First, the ventricular wall was labeled with DiI, and the positional relationship between transgene expression and the ventricular wall was evaluated. When transfected with PEI polyplexes, scarce ZsGreen1 expression was observed, only at the ventricular wall (Fig. 3A–C). As for pDNA + NBs and bubble lipopolyplexes combined with ultrasound irradiation, more transgene expression was observed (Fig. 3E, I), while ZsGreen1 expression was not detected without ultrasound irradiation (Fig. 3D, H). ZsGreen1 transfected by pDNA + NBs + US or bubble lipopolyplexes + US was observed at the ventricular wall (Fig. 3F, J) and choroid plexus (Fig. 3G, K). Apparently, more ZsGreen1 expression was observed at the choroid plexus than at the ventricular wall.

Next, to evaluate the positional relationship between blood vessels and transgene expression by pDNA + NBs or bubble lipopolyplexes combined with ultrasound, blood vessels were labeled by perfusion of DiI. In Fig. 4A and C, much ZsGreen1 expression obtained by both

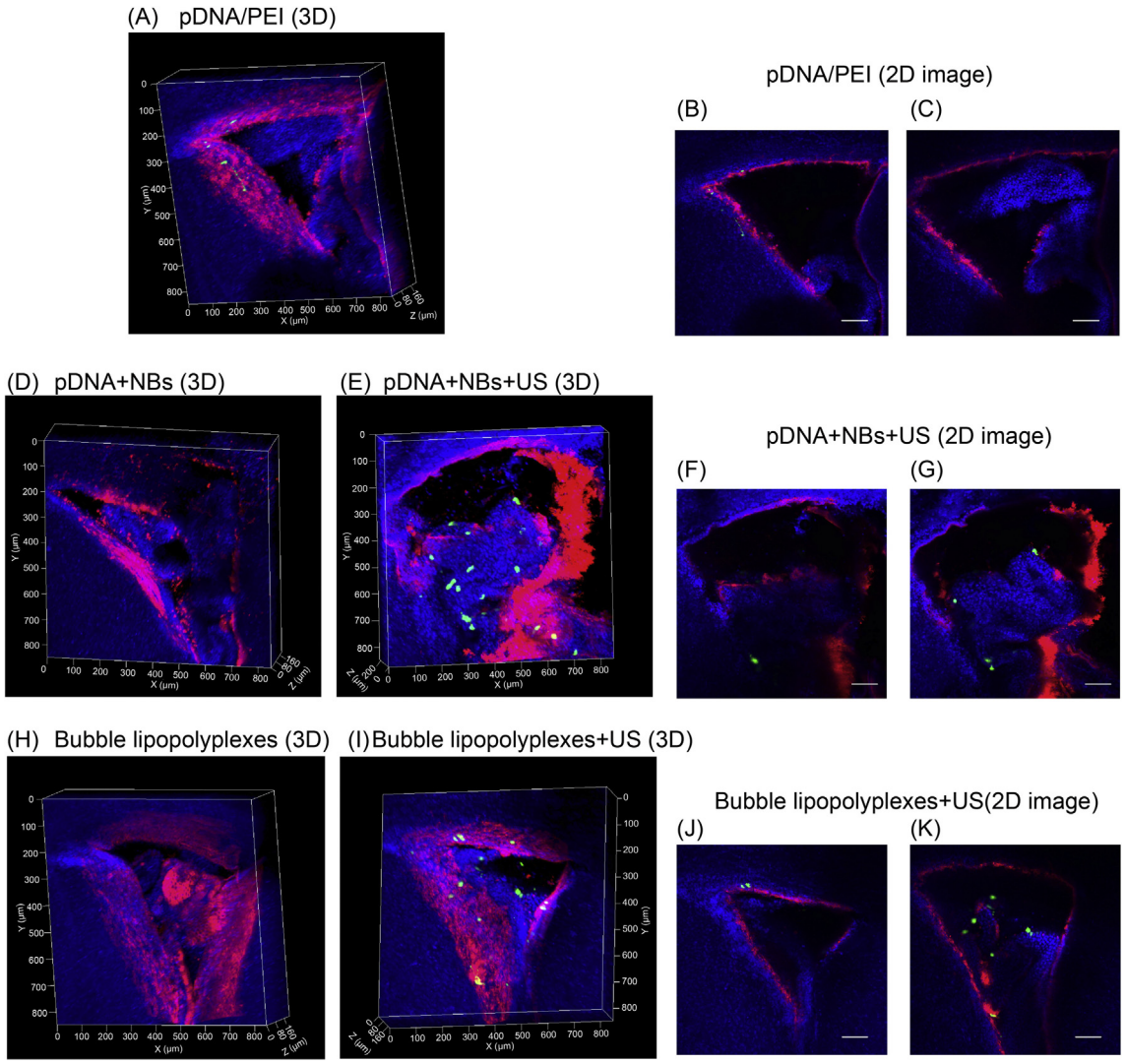

Fig. 3. Evaluation of spatial distribution of transgene expression using multicolor deep imaging. Twenty-four hours after ZsGreen1 transfection, ZsGreen1 expression around the left lateral ventricle was observed with confocal laser microscopy following staining of the ventricle walls by DiI and clearing with Sca*l*eSQ. (A, D, E, H, I) 3D images of ZsGreen1 expression transfected by each carrier (z-stack: 2 μm/slice, objective lens: 10 × dry lens). (B, C, F, G, J, K) Cross sections from each 3D image. Blue, green, and red represent DAPI, ZsGreen1, and DiI respectively. Scale bar = 100 μm. Abbreviation: 3D, 3-dimensional; 2D, 2-dimensional; NBs, nanobubbles; US, ultrasound; DAPI, 4′,6-diamidino-2-phenylindole; pDNA, plasmid DNA; PEI, polyethylenimine.

carriers was observed in the choroid plexus. When ZsGreen1-transfected choroid plexus was observed with high magnification, ZsGreen1 was expressed at cell layers outside the DiI-labeled choroid capillaries, which seem to be choroid epithelial cells. (Fig. 4B, 4D).

3.5. Assessment of tissue damage

After ultrasound-mediated transfection, tissue damage induction was analyzed using HE stain. Twenty-four hours after transfection, the ventricular wall and choroid plexus were observed. No morphological changes were detected in brains transfected with pDNA + NBs and bubble lipopolyplexes combined with ultrasound (Fig. 5C, D) when compared with PBS-injected control brains (Fig. 5B).

3.6. Sustainable secretion of lucia into CSF

CSF levels of secreted lucia were measured at 1, 7, 14 and 28 days after lucia was transfected with pDNA + NBs. At 1 day after transfection, lucia expression in mice irradiated with ultrasound was 600-fold higher than in mice without ultrasound irradiation (Fig. 6). Additionally, lucia expression in the CSF of ultrasound-irradiated mice was sustained, although the expression level decreased to about 1/10 over time (Fig. 6). At 7 days or later after transfection, lucia expression in mice without ultrasound irradiation was below the detectable limit (Fig. 6).

We also measured the lucia expression in serum at 1, 7, 14 and 28 days after transfection by pDNA + NBs. At all time points, lucia expression of both ultrasound-irradiated and non-irradiated mice was below the detectable limit (Data no shown).

4. Discussion

This study developed a method of ultrasound-mediated gene transfection to the cerebroventricular region via ICV administration of ultrasound-responsive NBs for therapeutic application. Tan et al [15] have reported the microbubbles and ultrasound-mediated gene transfection to the ventricular wall of the lateral ventricle; however, the influence of the ultrasound condition on the transfection efficiency has not been evaluated. Because these data are essential to obtain high transgene expression, we first measured the transgene expression using various ultrasound irradiation times and intensities, and then established the optimal ultrasound condition. Consequently, transgene

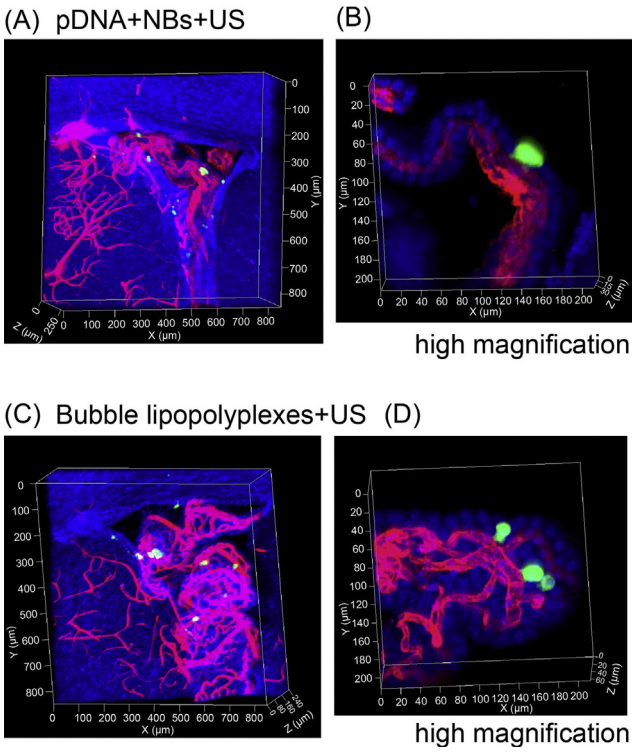

Fig. 4. Twenty-four hours after ZsGreen1 transfection, ZsGreen1 expression around the left lateral ventricle was observed with confocal laser microscopy following vascular staining by DiI and clearing with Sca*l*eSQ. (A, C) 3D images of ZsGreen1 expression transfected by each carrier (z-stack: 2 μm/slice, objective lens: 10 × dry lens). (B, D) High magnification 3D image (z-stack: 0.5 μm/slice, objective lens: 40 × oil immersion lens). Blue, green, and red represent DAPI, ZsGreen1, and DiI respectively. Abbreviation: US, ultrasound; pDNA, plasmid DNA; 3D, 3-dimensional; DAPI, 4′,6-diamidino-2-phenylindole.

expression by pDNA + NBs or bubble lipopolyplexes combined with ultrasound irradiation tended to be increased as irradiation time increased (Fig. 1A and C). Regarding the ultrasound intensity, transgene expression was drastically increased when ultrasound irradiated was conducted at 1 W/cm^2 (Fig. 1B and D), suggesting that 1 W/cm^2 was the threshold for ultrasound-mediated transgene expression. These results showed a similar trend to the data reported by Shimamura et al. [27], in which genes were transfected to brain by the injection of pDNA and microbubbles to the cisterna magna followed by ultrasound irradiation of the brain. These results suggest that both ultrasound duration and ultrasound intensity are controlling factors affecting the transgene expression of the ultrasound and bubble-mediated transfection. Based on the results, we expected that high transfection efficiency would be obtained with ultrasound irradiation for 60 sec at 1 W/cm^2; therefore we used this optimized condition in the following experiments.

PEI polyplexes are widely used for delivering pDNA or oligonucleotides to the cerebroventricular wall via ICV administration. We expected that ultrasound-mediated transfection exerts higher

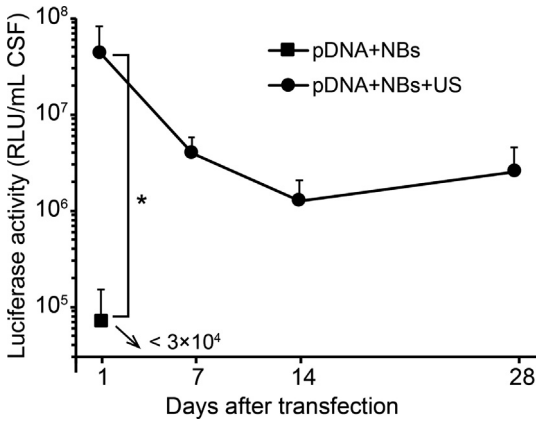

Fig. 6. Sustained transgene expression in CSF by CpG free vector. pCpG free-Lucia vector was transfected by pDNA + NBs and ultrasound irradiation. 1, 7, 14, and 28 days after transfection, CSF was collected from the cisterna magna. (n = 5) Data represent means ± SD. *$P < 0.05$, Student's *t*-test. Abbreviation: NBs, nanobubbles; pDNA, plasmid DNA; US, ultrasound; CSF, cerebrospinal fluid; SD, standard deviation.

transfection efficiency than PEI polyplexes in combination with external stimuli. Therefore, we compared the transfection efficiencies of PEI polyplexes and ultrasound-responsive carriers. Consequently, both pDNA + NBs and bubble lipopolyplexes combined with ultrasound showed significantly higher expression than PEI polyplexes, while transgene expression was extremely low when ultrasound was not irradiated (Fig. 2A, B). Next, we roughly evaluated the transfected area in the brain by dissecting into each area. High transgene expression was observed in the LH and RH, which contain lateral ventricles (Fig. 2C). On the other hand, little transgene expression was observed except in brain and spinal cord (Fig. 2C). These results suggest that highly efficient transgene expression is achieved selectively to brain by bubbles and ultrasound irradiation.

We are concerned with the comparison of pDNA + NBs and bubble lipopolyplexes because we and other researchers reported that the complex of pDNA and bubbles exerted high transfection efficiency compared with naked pDNA and bubbles in the case of intravenous carrier administration and ultrasound irradiation [12,28]. It is reported that the formation of a complex of pDNA and ultrasound-responsive bubbles increases the stability of pDNA by protecting it from DNase [29]. Moreover, complexation can integrate the behavior of each component. However, it is reported that CSF contains less DNase activity than serum does [30], and cerebral ventricles are small and closed region. Taking this into consideration, it is expected that the transfection efficiency is not improved by complexation of pDNA and NBs when carriers are administered via ICV. Expectedly, there were not big differences between transfection efficiency of pDNA + NBs and that of bubble lipopolyplexes in any brain areas (Fig. 2C). These findings suggest that complexation of pDNA and bubbles has little effect on the transfection efficiency in the ICV and ultrasound-mediated transfection to the cerebroventricular region.

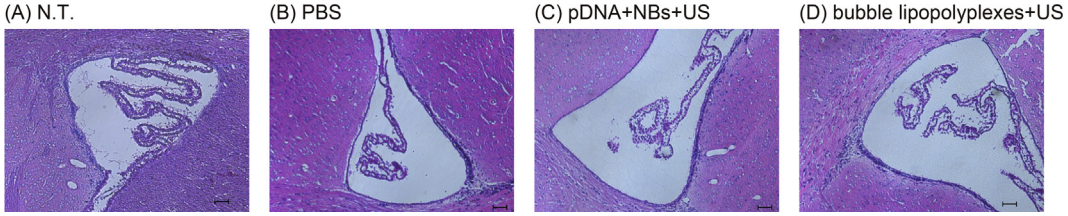

Fig. 5. Histological assessment with HE staining of the left ventricular wall and choroid plexus at twenty-four hours after transfection using pDNA + NBs or bubble lipopolyplexes combined with ultrasound irradiation. Objective lens: 10 × dry lens. Scale bar = 50 μm. Abbreviation: N.T., non-treatment; US, ultrasound; pDNA, plasmid DNA; HE, hematoxylin and eosin; NBs, nanobubbles.

Multicolor deep imaging is an observation system recently developed by our group that enables spatial and comprehensive observation with visualizing anatomical structures. Using this system, we evaluated the cerebral distribution of transgene expression obtained by pDNA + NBs and bubble lipopolyplexes combined with ultrasound irradiation to brain. First, the ventricular wall was visualized by labeling with DiI, and then transgene expression was observed. Consequently, PEI polyplex-mediated transgene expression was observed only at the ventricular wall (Fig. 3A–C). On the other hand, transgene expression by pDNA + NBs and bubble lipopolyplexes combined with ultrasound was also observed in the choroid plexus as well as at the ventricular wall (Fig. 3E-G, I-K). Moreover, more transgene-positive cells were observed in the choroid plexus than at the ventricular wall. We consider that the difference between transgene distribution of ultrasound-mediated expression and that of polyplex-mediated expression is caused by the different transfection mechanism. PEI polyplexes require contact with the cell membrane and internalization by endocytosis [31]. However, it might be difficult for PEI polyplexes to attach to the choroid plexus because the choroid plexus continuously secretes CSF. Therefore, PEI polyplexes-mediated transfection might be restricted to the ventricular wall. On the other hand, in the ultrasound and bubble-mediated transfection, contact with the cell surface is not necessarily required [32–34]. Therefore, genes may also be transfected to the choroid plexus. This is the first report to show ultrasound-mediated transgene expression, not only in the ventricular wall, but also in the choroid plexus. We believe that the spatial observation using multicolor deep imaging enabled detection of the transgene expression in the choroid plexus.

Next, transgene distribution in the choroid plexus was further investigated. We previously reported that intravenous injection of bubble lipopolyplexes and ultrasound irradiation to the brain transferred pDNA mainly to endothelial cells, which contain tight junctions [14]. Moreover, transfection to peritoneal tissues by intraperitoneal injection of pDNA + NBs and ultrasound irradiation resulted in transfection mainly to surface layers of peritoneal cells [11]. From these previous findings, it is expected that ultrasound-mediated transgene expression can be produced in the tissue closest to the bubbles. The choroid plexus consists of an inner fenestrated endothelial layer and outer choroid epithelial cell (CEC) layer which form the blood-cerebrospinal fluid barrier. Taking these into consideration, ultrasound-mediated transfection by ICV injection is expected to achieve transgene expression in CECs. To evaluate the positional relationship between choroid capillaries and transgene expression, we stained capillaries with DiI followed by tissue clearing. Consequently, transgene-positive cells were localized at the cell layer outside the DiI-labeled choroid capillaries (Fig. 4), which are expected to be CEC. This result suggests that ICV injection of bubbles combined with ultrasound irradiation is a CEC-targeted transfection system.

Tissue damage induced by ultrasound-mediated transfection is a concern for safe therapeutic application of this transfection system because the brain is sensitive to damage. In the ultrasound and bubble-mediated transfection to the brain via intravenous bubble administration, brain hemorrhage can be a serious problem [35–37]. However, the tissue damage to the cerebroventricular region induced by ultrasound-mediated transfection has not been evaluated. We evaluated the tissue damage with HE stain at 24 h after transfection. Consequently, few morphological changes and extravasations of red blood cells were observed in both pDNA + NBs + US and bubble lipopolyplexes + US compared to PBS-injected controls (Fig. 5A–D). These data suggest that ICV administration of ultrasound-responsive bubbles and ultrasound irradiation is a safe transfection system for the cerebroventricular region in terms of morphology and hemorrhage risk. Based on the results in this study, pDNA + NBs and bubble lipopolyplexes may not differ in transfection efficiency, transgene distribution, and tissue damage.

CECs secrete not only CSF but also proteins such as growth factors [38]. Recently, it has been reported that secreted proteins from CECs regulated the activation of NSCs in the SVZ [39]. In this study, we have revealed that ICV administration of bubbles and ultrasound irradiation brought about transgene expression in CECs. This result leads us to believe that ultrasound-mediated transfection of therapeutic genes encoding secretory protein to CECs and subsequent sustained secretion to the CSF is a feasible approach for treatment of cerebral diseases. Taking this into consideration, we evaluated the sustained transgene expression in CSF when the gene was transfected with pCpG free pDNA and NBs. Consequently, sustained gene expression in the CSF was observed for at least 28 days (Fig. 6). In contrast, secretory transgenic protein was not detected in the serum. This result is compatible with the findings reported by Hughes, T. S. et al [30], which showed sustainable transgenic protein secretion to the CSF by intrathecal administration of pCpG free pDNA. These results suggest that transfection of pCpG free vectors to CECs using ultrasound brings about the sustainable secretion of transgenic protein into CSF.

ICV administration is already clinically applied for injection of antibiotic agents or anticancer drugs by indwelling the Ommaya reservoir in brain [40]. Moreover, MRI-guided focused ultrasound irradiation device has been developed for the treatment of neurological diseases [41–44]. This device can irradiate precisely to the targeted region in the brain. By using the devise, it is expected that the selective gene transfection to choroid plexus may be achieved. We believe that the progress of such device enables us to apply the ultrasound-mediated gene transfection by ICV administration of nanobubbles for clinical gene therapy.

5. Conclusion

We successfully developed a method of ultrasound-responsive nanobubble-mediated gene transfection into the cerebroventricular region via ICV administration in mice. This transfection system efficiently transferred genes to CECs in the choroid plexus with no morphological change or hemorrhage. Moreover, we showed that sustained secretion of transgenic protein into the CSF was achieved using pCpG free vectors. We believe that this transfection system will offer a novel gene therapeutic method and gene functional analysis.

Acknowledgment

This work was a partly supported by JSPS KAKENHI Grant Number 16K18862 and 18H03535, the Shin-Nihon Foundation of Advanced Medical Research, and Takeda Science Foundation.

References

[1] C.B. Johansson, S. Momma, D.L. Clarke, M. Risling, Lendahl U, N JF. Identification of a neural stem cell in the adult mammalian central nervous system, Cell 96 (1999) 25–34.
[2] F. Doetsch, I. Caille, D.A. Lim, J.M. Garcia-Verdugo, A. Alvarez-Buylla, Subventricular zone astrocytes are neural stem cells in the adult mammalian brain, Cell 97 (1999) 703–716.
[3] C. Zhao, W. Deng, F.H. Gage, Mechanisms and functional implications of adult neurogenesis, Cell 132 (2008) 645–660.
[4] T. Ochi, H. Nakatomi, A. Ito, H. Imai, S. Okabe, N. Saito, Temporal changes in the response of SVZ neural stem cells to intraventricular administration of growth factors, Brain Res. 1636 (2016) 118–129.
[5] D. Goula, J.S. Remy, P. Erbacher, M. Wasowicz, G. Levi, B. Abdallah, B.A. Demeneix, Size, diffusibility and transfection performance of linear PEI/DNA complexes in the mouse central nervous system, Gene Ther. 5 (1998) 712–717.
[6] G.F. Lemkine, S. Mantero, C. Migne, A. Raji, D. Goula, P. Normandie, G. Levi, B.A. Demeneix, Preferential transfection of adult mouse neural stem cells and their immediate progeny in vivo with polyethylenimine, Mol. Cell. Neurosci. 19 (2002) 165–174.
[7] B. Newland, T.C. Moloney, G. Fontana, S. Browne, M.T. Abu-Rub, E. Dowd, A.S. Pandit, The neurotoxicity of gene vectors and its amelioration by packaging with collagen hollow spheres, Biomaterials 34 (2013) 2130–2141.
[8] Y. Liu, H. Miyoshi, M. Nakamura, Encapsulated ultrasound microbubbles: therapeutic application in drug/gene delivery, J. Control Release 114 (2006) 89–99.
[9] R. Suzuki, T. Takizawa, Y. Negishi, K. Hagisawa, K. Tanaka, K. Sawamura, N. Utoguchi, T. Nishioka, K. Maruyama, Gene delivery by combination of novel

liposomal bubbles with perfluoropropane and ultrasound, J. Control Release 117 (2007) 130–136.
[10] K. Maruyama, R. Suzuki, J. Unga, D. Omata, Y. Oda, Theranostic bubble preparation (TB), and method for using same. PCTJP2016002810 (2016).
[11] K. Nishimura, S. Fumoto, Y. Fuchigami, M. Hagimori, K. Maruyama, S. Kawakami, Effective intraperitoneal gene delivery system using nanobubbles and ultrasound irradiation, Drug Deliv. 24 (2017) 737–744.
[12] K. Un, S. Kawakami, R. Suzuki, K. Maruyama, F. Yamashita, M. Hashida, Development of an ultrasound-responsive and mannose-modified gene carrier for DNA vaccine therapy, Biomaterials. 31 (2010) 7813–7826.
[13] T. Kurosaki, S. Kawakami, Y. Higuchi, R. Suzuki, K. Maruyama, H. Sasaki, F. Yamashita, M. Hashida, Development of anionic bubble lipopolyplexes for efficient and safe gene transfection with ultrasound exposure in mice, J. Control Release 176 (2014) 24–34.
[14] K. Ogawa, Y. Fuchigami, M. Hagimori, S. Fumoto, Y. Miura, S. Kawakami, Efficient gene transfection to the brain with ultrasound irradiation in mice using stabilized bubble lipopolyplexes prepared by the surface charge regulation method, Int. J. Nanomedicine 13 (2018) 2309–2320.
[15] J.Y. Tan, B. Pham, Y. Zong, C. Perez, D.O. Maris, A. Hemphill, C.H. Miao, T.J. Matula, P.D. Mourad, H. Wei, D.L. Sellers, P.J. Horner, S.H. Pun, Microbubbles and ultrasound increase intraventricular polyplex gene transfer to the brain, J. Control Release 231 (2016) 86–93.
[16] S. Fumoto, K. Nishimura, K. Nishida, S. Kawakami, Three-dimensional imaging of the intracellular fate of plasmid DNA and transgene expression: ZsGreen1 and tissue clearing method CUBIC are an optimal combination for multicolor deep imaging in murine tissues, PLoS One 11 (2016) e0148233.
[17] N. Oyama, Y. Fuchigami, S. Fumoto, M. Sato, M. Hagimori, K. Shimizu, S. Kawakami, Characterization of transgene expression and pDNA distriburion of suctioned kidney in mice, Drug Deliv. 24 (2017) 906–917.
[18] A. Haraguchi, Y. Fuchigami, M. Kawaguchi, S. Fumoto, K. Ohyama, K. Shimizu, M. Hagimori, S. Kawakami, Determining transgene expression characteristics using a suction device with multiple hole adjusting a left lateral lobe of the mouse liver, Biol. Pharm. Bull. 41 (2018) 944–950.
[19] T. Suga, N. Kato, M. Hagimori, Y. Fuchigami, N. Kuroda, Y. Kodama, H. Sasaki, S. Kawakami, Development of high-functionality and -quality Lipids with RGD peptide ligands: application for PEGylated liposomes and analysis of intratumoral distribution in a murine colon cancer model, Mol. Pharm. 15 (2018) 4481–4490.
[20] T. Nomura, K. Yasuda, T. Yamada, S. Okamoto, R.I. Mahato, Y. Watanabe, Y. Takakura, M. Hashida, Gene expression and antitumor effects following direct interferon (IFN)-γ gene transfer with naked plasmid DNA and DC-chol liposome complexes in mice, Gene Ther. 6 (1999) 121–129.
[21] Y. Miura, Y. Fuchigami, M. Hagimori, H. Sato, K. Ogawa, C. Munakata, M. Wada, K. Maruyama, S. Kawakami, Evaluation of the targeted delivery of 5-fluorouracil and ascorbic acid into the brain with ultrasound-responsive nanobubbles, J. Drug Target. 26 (2018) 684–691.
[22] S. Kawai, Y. Takagi, S. Kaneko, T. Kurosawa, Effect of three types of mixed anesthetic agents alternate to ketamine in mice, Exp. Anim. 60 (2011) 481–487.
[23] E.J. Kwon, J. Lasiene, B.E. Jacobson, I.K. Park, P.J. Horner, S.H. Pun, Targeted nonviral delivery vehicles to neural progenitor cells in the mouse subventricular zone, Biomaterials 31 (2010) 2417–2424.
[24] L. Liu, K. Duff, A technique for serial collection of cerebrospinal fluid from the cisterna magna in mouse, J. Vis. Exp. 21 (2008) e960.
[25] H. Hama, H. Hioki, K. Namiki, T. Hoshida, H. Kurokawa, F. Ishidate, T. Kaneko, T. Akagi, T. Saito, T. Saido, A. Miyawaki, *ScaleS*: an optical clearing palette for biological imaging, Nat. Neurosci. 18 (2015) 1518–1529.
[26] Y. Li, Y. Song, L. Zhao, G. Gaidosh, A.M. Laties, R. Wen, Direct labeling and visualization of blood vessels with lipophilic carbocyanine dye DiI, Nat Protoc. 3 (2008) 1703–1708.
[27] M. Shimamura, N. Sato, Y. Taniyama, S. Yamamoto, M. Endoh, H. Kurinami, M. Aoki, T. Ogihara, Y. Kaneda, R. Morishita, Development of efficient plasmid DNA transfer into adult rat central nervous system using microbubble-enhanced ultrasound, Gene Ther. 11 (2004) 1532–1539.
[28] D.S. Wang, C. Panje, M.A. Pysz, R. Paulmurugan, J. Rosenberg, S.S. Gambhir, M. Schneider, J.K. Willmann, Cationic versus neutral microbubbles for ultrasound-mediated gene delivery in cancer, Radiology 264 (2012) 721–732.
[29] C.M. Panje, D.S. Wang, M.A. Pysz, R. Paulmurugan, Y. Ren, F. Tranquart, L. Tian, J.K. Willmann, Ultrasound-mediated gene delivery with cationic versus neutral microbubbles: effect of DNA and microbubble dose on in vivo transfection efficiency, Theranostics 2 (2012) 1078–1091.
[30] T.S. Hughes, S.J. Langer, K.W. Johnson, R.A. Chavez, L.R. Watkins, E.D. Milligan, L.A. Leinwand, Intrathecal injection of naked plasmid DNA provides long-term expression of secreted proteins, Mol. Ther. 17 (2009) 88–94.
[31] J. Rejman, A. Bragonzi, M. Conese, Role of clathrin- and caveolae-mediated endocytosis in gene transfer mediated by lipo- and polyplexes, Mol. Ther. 12 (2005) 468–474.
[32] A. Delalande, S. Kotopoulis, M. Postema, P. Midoux, C. Pichon, Sonoporation: mechanistic insights and ongoing challenges for gene transfer, Gene 525 (2013) 191–199.
[33] H. Fu, J. Comer, W. Cai, C. Chipot, Sonoporation at small and large length scales: effect of cavitation bubble collapse on membranes, J. Phys. Chem. Lett. 6 (2015) 413–418.
[34] M. Wang, Y. Zhang, C. Cai, J. Tu, X. Guo, D. Zhang, Sonoporation-induced cell membrane permeabilization and cytoskeleton disassembly at varied acoustic and microbubble-cell parameters, Sci. Rep. 8 (2018) 3885.
[35] Q. Huang, J. Deng, Z. Xie, F. Wang, S. Chen, B. Lei, P. Liao, N. Huang, Z. Wang, Z. Wang, Y. Cheng, Effective gene transfer into central nervous system following ultrasound-microbubbles-induced opening of the blood-brain barrier, Ultrasound Med. Biol. 38 (2012) 1234–1243.
[36] H.B. Wang, L. Yang, J. Wu, L. Sun, J. Wu, H. Tian, R.D. Weisel, R.K. Li, Reduced ischemic injury after stroke in mice by angiogenic gene delivery via ultrasound-targeted microbubble destruction, J. Neuropathol. Exp. Neurol. 73 (2014) 548–558.
[37] B.P. Mead, P. Mastorakos, J.S. Suk, A.L. Klibanov, J. Hanes, R.J. Price, Targeted gene transfer to the brain via the delivery of brain-penetrating DNA nanoparticles with focused ultrasound, J. Control Release 223 (2016) 109–117.
[38] E. Thouvenot, M. Lafon-Cazal, E. Demettre, P. Jouin, J. Bockaert, P. Marin, The proteomic analysis of mouse choroid plexus secretome reveals a high protein secretion capacity of choroidal epithelial cells, Proteomics 6 (2006) 5941–5952.
[39] V. Silva-Vargas, A.R. Maldonado-Soto, D. Mizrak, P. Codega, F. Doetsch, Age-dependent niche signals from the choroid plexus regulate adult neural stem cells, Cell Stem Cell 19 (2016) 643–652.
[40] I. Slavc, J.L. Cohen-Pfeffer, S. Gururangan, J. Krauser, D.A. Lim, M. Maldaun, C. Schwering, A.J. Shaywitz, M. Westphal, Best practices for the use of intracerebroventricular drug delivery devices, Mol. Genet. Metab. Rep. 124 (2018) 184–188.
[41] E. Martin, D. Jeanmonod, A. Morel, E. Zadicario, B. Werner, High-intensity focused ultrasound for noninvasive functional neurosurgery, Ann. Neurol. 66 (2009) 858–861.
[42] S.R. Schreglmann, R. Bauer, S. Hägele-Link, K.P. Bhatia, P. Natchev, N. Wegener, A. Lebeda, B. Werner, E. Martin, G. Kägi, Unilateral cerebellothalamic tract ablation in essential tremor by MRI-guided focused ultrasound, Neurology 88 (2017) 1329.
[43] G. Toccaceli, R. Delfini, C. Colonnese, A. Raco, S. Peschillo, Emerging strategies and future perspective in neuro-oncology using transcranial focused ultrasonography technology, World Neurosurgery 117 (2018) 84–91.
[44] G. Toccaceli, G. Barbagallo, S. Peschillo, Low-intensity focused ultrasound for the treatment of brain diseases: safety and feasibility, Theranostics 9 (2019) 537–539.